PERIOD2::LUCIFERASE real-time reporting of circadian dynamics reveals persistent circadian oscillations in mouse peripheral tissues

Seung-Hee Yoo*†, Shin Yamazaki‡§, Phillip L. Lowrey*¶, Kazuhiro Shimomura*¶‖, Caroline H. Ko*,**, Ethan D. Buhr*, Sandra M. Siepka¶‖, Hee-Kyung Hong*¶, Won Jun Oh†, Ook Joon Yoo†, Michael Menaker‡, and Joseph S. Takahashi*¶††

¶Howard Hughes Medical Institute, *Department of Neurobiology and Physiology, and ‖Center for Functional Genomics, Northwestern University, 2205 Tech Drive, Evanston, IL 60208; ‡National Science Foundation Center for Biological Timing and Department of Biology, University of Virginia, Charlottesville, VA 22904; †Department of Biological Sciences, Korea Advanced Institute of Science and Technology, Taejon 305-701, Korea; and **Department of Psychology, University of Toronto, Toronto, ON, Canada M5S 3G3

This contribution is part of the special series of Inaugural Articles by members of the National Academy of Sciences elected on April 29, 2003.

Contributed by Joseph S. Takahashi, December 30, 2003

Mammalian circadian rhythms are regulated by the suprachiasmatic nucleus (SCN), and current dogma holds that the SCN is required for the expression of circadian rhythms in peripheral tissues. Using a PERIOD2::LUCIFERASE fusion protein as a real-time reporter of circadian dynamics in mice, we report that, contrary to previous work, peripheral tissues are capable of self-sustained circadian oscillations for >20 cycles in isolation. In addition, peripheral organs expressed tissue-specific differences in circadian period and phase. Surprisingly, lesions of the SCN in *mPer2*^{Luciferase} knockin mice did not abolish circadian rhythms in peripheral tissues, but instead caused phase desynchrony among the tissues of individual animals and from animal to animal. These results demonstrate that peripheral tissues express self-sustained, rather than damped, circadian oscillations and suggest the existence of organ-specific synchronizers of circadian rhythms at the cell and tissue level.

In mammals, a circadian pacemaker located in the suprachiasmatic nucleus (SCN) of the anterior hypothalamus rests at the top of a circadian hierarchy to drive circadian rhythms of behavior and activity at the organismal level (1–4). In multicellular organisms, it has become clear that, in addition to circadian pacemakers located in the CNS, there are oscillators in peripheral tissues (5–8). Perhaps the most compelling example is the discovery that Rat-1 fibroblasts are capable of circadian gene expression after serum stimulation (9). Currently, a wide range of peripheral tissues has been shown to have some capacity for circadian oscillations; however, in all such cases, there appears to be a dichotomy between the SCN and peripheral oscillators. The SCN can express persistent, self-sustained oscillations (>30 cycles in isolation), whereas peripheral rhythms damp out after two to seven cycles (7). This finding has led to a widely accepted hierarchical model of the mammalian circadian system in which the SCN acts as a pacemaker, independently able to both generate and sustain its own circadian oscillations, and necessary to drive circadian oscillations in peripheral cells of neural and non-neural origin (4, 7, 8, 10). Consistent with this model is the observation that peak expression of core circadian genes in peripheral tissues is phase-delayed by 3–9 h relative to their maximal expression in the SCN, suggesting that the SCN phase leads and drives the peripheral circadian rhythms (11–13). Furthermore, in the absence of the SCN, whether by lesioning this structure in the living animal or *ex vivo* culturing of peripheral tissues, rhythms in circadian gene expression damp after two to seven cycles (7, 14, 15).

To address whether the persistence of circadian rhythms differs in peripheral tissues as compared to the SCN, we have used the mouse *Period2* (*mPer2*) locus to create a real-time gene expression reporter of circadian dynamics. Here, we report the generation of *mPer2*^{Luciferase} (*mPer2*^{Luc}) knockin mice in which a *Luc* gene is fused in-frame to the 3′ end of the endogenous *mPer2* gene. Previous work from a number of laboratories using the *mPer1* (rather than the *mPer2*) locus has shown that the SCN expresses persistent circadian rhythms in reporter gene activity, whereas peripheral organs fail to do so (7, 16–18). In contrast, in *mPer2*^{Luc} mice, we find that both SCN and peripheral tissues in explant cultures show robust and self-sustained circadian rhythms for at least 20 days. Furthermore, in SCN-lesioned *mPer2*^{Luc} mice, we observe a persistent circadian oscillation in bioluminescence in peripheral tissues, yet from tissue to tissue within each animal and among animals, a gradual loss of phase coordination develops. These results demonstrate that peripheral tissues contain self-sustained circadian oscillators that are as robust as those found in the SCN. Furthermore, the long-term persistence of the oscillations suggests the existence of previously unrecognized synchronizing mechanisms in peripheral organs.

Materials and Methods

Generation of *mPer2*^{Luc} Knockin Mice. A mouse bacterial artificial chromosome (BAC) library (CitbCJ7, Research Genetics, Huntsville, AL) generated from 129Sv embryonic stem (ES) cells was screened with a full-length *mPer2* cDNA probe. A 15.9-kb *Eco*RI fragment was isolated from one of six positively hybridizing BAC clones and was partially digested with *Xma*I to yield a 6.4-kb fragment, which was subsequently ligated in-frame to a 1.7-kb PCR-amplified *Luc* gene (pGL3-Basic vector; Promega). The resulting 8.1- and 3-kb fragments from the 3′ UTR of the *mPer2* gene were used as the long and short arms of the targeting construct, respectively, in the pKO Scrambler 916 vector (Lexicon, The Woodlands, TX). For positive and negative selection, the diphtheria toxin A chain (pKO Select vector; Lexicon) and a neomycin gene flanked by lox P sites (a gift of A. L. Joyner, New York University School of Medicine, New York) were used. Homologous recombinants were isolated after electroporation with 40 μg of targeting construct into 2×10^7 W4 ES cells (129S6SvEvTac; provided by A. L. Joyner). After G418 selection (200 μg/ml), ≈400 surviving clones were screened by Southern analysis to detect homologous recombinants. A 600-bp

Abbreviations: Per2, Period2; Luc, luciferase; SCN, suprachiasmatic nucleus; ES, embryonic stem; LD12:12, 12-h light/12-h dark cycle; DD, constant darkness; PMT, photomultiplier tube.

See accompanying Biography on page 5336.

§Present address: Department of Biological Sciences, Vanderbilt University, Box 1634-B, Nashville, TN 37235-1634.

††To whom correspondence should be addressed. E-mail: j-takahashi@northwestern.edu.

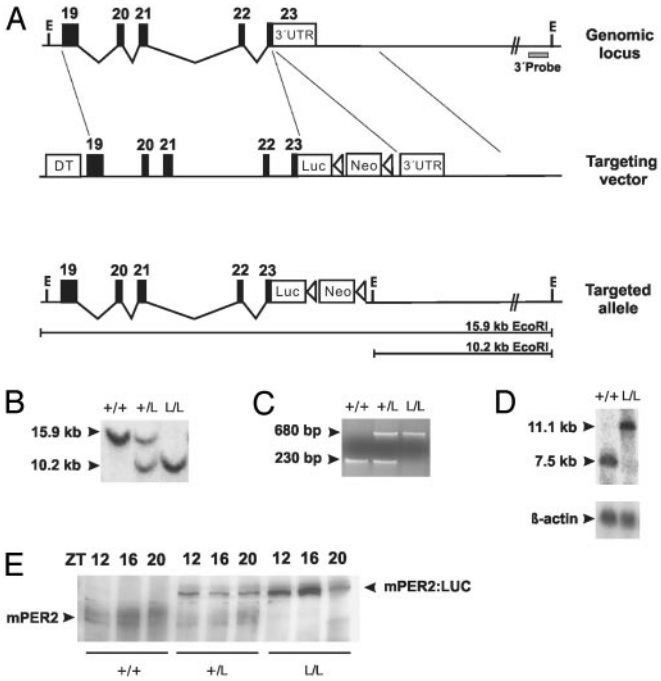

Fig. 1. Generation of *mPer2*^{Luc} knockin mice. (*A*) Diagram of the *mPer2* locus, targeting vector, and targeted knockin allele. Exons are indicated by filled blocks with numbers. E, *Eco*RI; DT, diphtheria toxin A chain; Neo, neomycin resistance gene; triangle, loxP site. (*B*) Southern blot of DNA from F_2 animals after digestion with *Eco*RI. The 600-bp 3′ external probe (*A*) detects a 15.9-kb WT fragment and a 10.2-kb targeted fragment. + indicates WT; L indicates *luc* knockin allele. (*C*) PCR genotyping of F_2 animals. Agarose gel electrophoresis reveals the presence of a 230-bp WT (+) allele and a 680-bp knockin allele (L). (*D*) Northern blot of total RNA extracted from mouse brain probed with a 1.4-kb *mPer2* partial cDNA fragment. In contrast to the 7.5-kb WT (+) allele, the larger 11.1-kb band represents the transcript from the targeted (L) allele. (*E*) Western blot of WT (+/+), *mPer2*^{Luc} heterozygote (+/L), and homozygote (L/L) mouse.

PCR probe to the 3′ end of the genomic *mPer2* locus was amplified from C57BL/6J mouse genomic DNA by using the following primers: (forward) 5′-GTCCTCCGGTGTTTTAGGATTT-3′ and (reverse) 5′-GGTGCATGAAATAATGGGGTAG-3′. These and all subsequent primers were synthesized by Integrated DNA Technologies (Coralville, IA). Probes were labeled with [α-^{32}P]dCTP (6,000 Ci/mmol, NEN Research Products) by using the Megaprime DNA Labeling System (Amersham Pharmacia). Targeted ES cell clones were injected into C57BL/6J blastocysts and transferred to pseudopregnant C57BL/6J female recipients. Resulting male chimeras were bred with C57BL/6J females. Germ-line transmission was confirmed by agouti coat color and Southern analysis using the 3′ *mPer2* probe described above (Fig. 1*A*). F_1 and F_2 offspring from an F_1 intercross were used for all subsequent experiments. To distinguish between heterozygous and homozygous knockin animals, PCR genotyping was performed by using 5′-CTGTGTTTACTGCGAGAGT-3′ (P1) and 5′-GGGTCCATGTGATTAGAAAC-3′ (P2) as WT allele detection primers and 5′-TAAAACCGGGAGGTAGATGAGA-3′ (P3) as a reverse primer with P1 for the *Luc* knockin allele detection (Fig. 1*C*). The P2 region is deleted in the targeted allele. PCR was performed on tail genomic DNA for 35 cycles of 95°C at 1 min, 55°C at 1 min, and 72°C at 1 min using AmpliTaq DNA polymerase (Applied Biosystems). For Northern analysis, commercially available reagents were used (RNAqueous Kit and NorthernMax Reagents, Ambion, Austin, TX) following the manufacturer's protocols. Total RNA was isolated from whole mouse brain, and DNA probes were generated from C57BL/6J *mPer2* cDNA. For Western blot analysis, kidney tissues were removed at ZT12, ZT16, and ZT20 from *mPer2*^{Luc} homozygous, heterozygous, and WT littermates, dissected, and frozen on dry ice. Tissues were homogenized at 4°C in 3 vol of lysis buffer (0.4 M NaCl/20 mM Hepes, pH 7.5/1 mM EDTA/1 mM DTT/0.3% Triton X-100/0.25 mM PMSF/10 mg/ml aprotinin/5 mg/ml leupeptin/1 mg/ml pepstatin A). Homogenates were cleared by centrifugation for 20 min at 13,000 rpm. One hundred micrograms of protein per lane was separated by electrophoresis by 6% polyacrylamide-SDS gels and then transferred to poly(vinylidene difluoride) membranes. Five percent nonfat dry milk in Tris-buffered saline containing 0.05% Tween 20 was used for blocking. mPER2 rat antibody was generously provided by Steven Reppert (University of Massachusetts Medical School, Worcester). Immunoreactive bands were visualized by using anti-rat IgG secondary antisera (Jackson ImmunoResearch) and Western blotting lumonol reagent (Santa Cruz Biotechnology).

Animals. Mice were bred from *mPer2*^{Luc} heterozygotes from (129SvEv × C57BL/6J)F_1 parents at Northwestern University. F_2 animals were raised in a 12-h light/12-h dark cycle (LD12:12) from birth. After weaning, animals were group-housed (one to five mice per cage), and at 8–12 weeks of age they were transferred into individual cages equipped with running wheels in LD12:12. After a minimum of 7 days entrainment to LD12:12, animals were transferred into constant darkness (DD) for 3 weeks. Mice were again transferred to LD12:12 for 3 weeks, followed by another 3-week DD exposure. Six-hour light pulses (fluorescent light, ≈300 lux) were given at circadian time 16 (4 h after activity onset) on day 21 during the second DD exposure. Animals were then returned to DD for 2 weeks. For bioluminescence monitoring, animals were transferred to the University of Virginia and maintained on light cycles as described above for at least 2 weeks before experiments. All animal studies were conducted in accordance with the regulations of the Committee on Animal Care and Use at Northwestern University and the University of Virginia.

Circadian Activity Analysis. Wheel-running activity was recorded and analyzed as described (19–21). Activity data were recorded continuously by a PC system (Chronobiology Kit, Stanford Software Systems, Santa Cruz, CA) and displayed and analyzed by using CLOCKLAB software (Actimetrics, Evanston, IL). The free-running period was calculated (days 1–20 in DD) by using a χ^2 periodogram (22) with 6-min resolution between 10 and 36 h (CLOCKLAB). The magnitude of phase shifts was determined by measuring the phase difference, based on the activity onset as a phase reference point, between eye-fitted regression lines between three and seven consecutive activity-onset times immediately before the light pulse, and at least seven consecutive activity-onset times after the light pulse (excluding the four cycles immediately after the pulse). The amplitude of the circadian component was estimated from a normalized Fourier spectrum by using 20 days in DD (CLOCKLAB). Original data were collected at 1-min intervals. To prepare the power spectra, data points were first binned into 6-min intervals, for a total of 3,600 bins for the 20-day period to be analyzed. A fourth-order Blackman–Harris window was then applied to these points before calculating the power spectrum by using fast Fourier transform as described (23). The spectrum was normalized to an integral of one by dividing each of its elements by the sum of all elements. For each animal the frequency of the spectrum peak is reported, along with the amplitude of the peak, which represents the relative power within a frequency band of 0.0028. The total number of running-wheel revolutions was counted from days 1 to 20 in DD and then averaged to determine the daily activity level.

SCN Lesions. SCN lesions were performed on 7- to 12-week-old homozygous or heterozygous *mPer2*^{Luc} knockin mice maintained on an LD12:12 cycle. Animals were anesthetized with Ketamine (80 μg/g of body mass) and Xylazine (0.4 μg/g of body mass) i.p. and placed in a stereotaxic apparatus (Kopf Instruments, Tujunga, CA). The height of the tooth bar was set at 0.0 mm relative to the ear bar. The electrode (RNE-300X, Rhodes Medical Instruments, Woodland, CA) was positioned in the middle of the midsagittal sinus, 0.4 mm anterior to bregma. The electrode position was marked, a small hole was drilled through the skull, and the electrode was slowly lowered vertically to the desired depth of 6.0 mm below the skull. Lesions were made by passing a constant current of 2 mA for 10 s (D.C. Constant Lesion Maker, model D.C. LM5, Grass Instruments, Quincy, MA). After 7–10 days of postsurgical recovery, mice were tested for circadian locomotor activity rhythms. Mice exhibiting arrhythmic locomotor activity in DD were subsequently used for tissue explant studies at 12, 16, and 32 days after DD exposure. Tissue explants were also obtained from intact control animals housed in DD.

Explant Cultures. Approximately 1 h before lights off, mice were anesthetized with CO_2 and decapitated, and their brains were rapidly removed. The pituitary was excised from the brain and immediately placed in cold Hank's balanced salt solution (HBSS, Invitrogen). Coronal sections of the brain (300-μm thickness) made with a Vibratome were transferred to cold HBSS. Brain regions were identified under a dissecting microscope and isolated as square tissues ≈1.5 mm across with a pair of scalpels. The SCN and retrochiasmatic area were dissected and cultured separately on Millicell culture membranes (PICM ORG 50, Millipore) with 1.2 ml DMEM (Invitrogen), supplemented with 10 mM Hepes (pH 7.2), 2% B27 (Invitrogen), 25 units/ml penicillin, 25 μg/ml streptomycin, and 0.1 mM luciferin (Promega). Whole pituitaries were flattened and placed on the plate inserts. Peripheral tissue sections (1-mm thickness, liver, lung, and kidney) and whole corneas were cultured as above, but without the Millicell membrane. For SCN-lesioned animals, mice were killed in DD by decapitation under Halothane anesthesia with an IR viewer (FJW Optical Systems, Palatine, IL). After removal of both eyeballs, peripheral tissues were removed under red safelights. The cornea, pituitary, liver, lung, and kidney were explanted as described above. Individual tissue cultures were sealed in 35-mm Petri dishes with a coverslip and vacuum grease. Cultures were maintained at 36°C in a light-tight, water-jacketed incubator, and their bioluminescence was continuously monitored with photomultiplier tube (PMT) detector assemblies (HC135-11 MOD, Hamamatsu, Bridgewater, NJ). The PMT was positioned ≈1 cm above each culture, and photon counts were integrated over 1-min intervals. Dark counts (nonspecific counts) from the PMTs were ≈20 to 40 counts per s at 36°C. Light emission from cultured tissues was measured immediately upon placement in culture without interruption for >7 days.

Bioluminescence Data Analysis. Period and phase measurements were calculated as in previous studies (8, 24, 25). Briefly, the original data (1-min bins) were smoothed by an adjacent-averaging method with 2-hr running means. The peak was calculated as the highest point of smoothed data, and the free-running period was computed as the mean between the peaks in each cycle.

Results and Discussion

Gene Targeting of the *mPer2* Locus to Create a PER2::LUC Fusion Reporter Mouse. Because null mutations of the *mPer2* locus have been shown to affect the circadian phenotype of mice and because circadian rhythms of *mPer2* mRNA and protein levels are extremely robust, we chose this gene to create a unique circadian reporter in mouse. We used a knock-in approach in which a firefly *Luc* gene was fused to the terminal exon of the endogenous *mPer2* locus by means of homologous recombination in ES cells to create a fusion protein reporter for two reasons. First, we could preserve both proximal and distal regulatory elements that could have been inadvertently omitted in conventional transgenic constructs. Second, by creating an mPER2::LUC fusion protein, we could follow the dynamical consequences of both transcriptional and posttranscriptional regulation of the mPER2 protein. To this end, we isolated a 6.4-kb *Eco*RI/*Xma*I DNA fragment containing *mPer2* exons 19–23 (minus the last 24 aa encoded by exon 23) from a mouse bacterial artificial chromosome genomic library and fused it in-frame to the *Luc* gene. The resulting 8.1-kb fragment was used as the long arm of our targeting construct (Fig. 1*A*). Presence of the targeted allele was confirmed in two ways: Southern analysis (Fig. 1*B*) and PCR (Fig. 1*C*). Northern analysis revealed equivalent levels of 7.5- and 11.1-kb *mPer2* transcripts from WT and homozygous *mPer2*^{Luc} mice, respectively, consistent with the expected size of the *mPer2*^{Luc} transcript (Fig. 1*D*). Western blotting was performed to confirm the expression of the mPER2::LUC fusion protein (Fig. 1*E*). Antibody against mPER2 detected both the endogenous mPER2 protein and the mPER2::LUC fusion protein during their peak expression times from WT, heterozygous knockin, and homozygous knockin littermates. Intercrosses between heterozygous (C57BL/6J × 129S6SvEvTac)F_1 offspring produced WT, heterozygous *mPer2*^{Luc} knockin, and homozygous *mPer2*^{Luc} knockin F_2 animals at the expected 1:2:1 Mendelian ratios. Mice heterozygous and homozygous for the targeted allele were developmentally and morphologically indistinguishable from WT littermates.

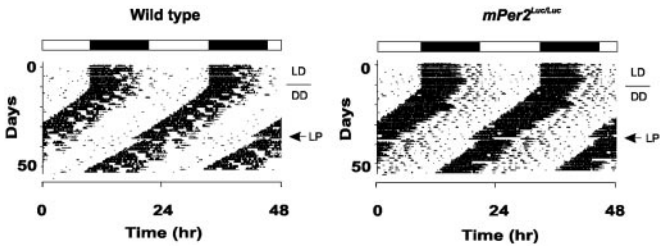

Fig. 2. Representative locomotor activity records from WT and *mPer2*$^{Luc/Luc}$ homozygous knockin mice. Animals were maintained on LD12:12 for the first 10 days, indicated by the filled and empty bars above the records, before transfer to DD to measure free-running period. On day 22 in DD conditions, a 6-h light pulse (LP; arrow) was administered at circadian time 16.

To determine whether the mPER2::LUC fusion protein was functional *in vivo*, we analyzed the circadian behavior of *mPer2*^{Luc} knockin mice. Because a null mutation of the *mPer2* locus causes period shortening and a loss of circadian rhythms in DD (26), we specifically tested for these phenotypic effects. There were no differences in the entrainment of *mPer2*^{Luc} mice to LD12:12. In DD, four different circadian traits were examined that reflect fundamental properties of circadian pacemakers: free-running period, amplitude of circadian rhythms, daily activity levels, and the magnitude of light-induced phase shifts. As shown in Fig. 2 and Table 1, no significant differences were detected among WT, heterozygous, or homozygous *mPer2*^{Luc} knockin mice in any of the four parameters, demonstrating that the mPER2::LUC fusion protein can completely rescue the function of the WT mPER2 protein with respect to its role in circadian locomotor behavior.

Tissue-Specific Circadian Expression of mPER2::LUC. To monitor circadian dynamics in different tissues, luminescence was continuously measured in real time with PMT detectors. After

Table 1. Circadian phenotypic characteristics of *mPer2*^{Luc} mice

Mice	Parameter	ANOVA *n*	ANOVA *F* value	ANOVA *P* value
	Period, hr			
+/+	23.56 ± 0.12	7	0.45	0.64
Luc/+	23.61 ± 0.09	10		
Luc/*Luc*	23.69 ± 0.07	7		
	Amplitude, %			
+/+	12.13 ± 2.63	7	1.53	0.24
Luc/+	10.54 ± 1.28	10		
Luc/*Luc*	14.67 ± 1.65	7		
	Daily activity, rev × 10^4			
+/+	2.85 ± 0.59	7	0.53	0.59
Luc/+	2.43 ± 0.32	10		
Luc/*Luc*	2.91 ± 0.29	7		
	Phase shift, hr			
+/+	−4.29 ± 0.64	5	0.70	0.51
Luc/+	−3.60 ± 0.60	8		
Luc/*Luc*	−3.16 ± 0.79	6		

Values are presented as mean ± SEM. Effects of genotype were analyzed by one-way ANOVA. See *Materials and Methods* for analysis of circadian phenotypes.

entrainment of *mPer2*^{Luc} knockin animals to an LD12:12, SCN, neural, and peripheral tissues were dissected and placed in static cultures containing media supplemented with luciferin substrate, and luminescence was measured for an initial period of ≈7 days (Fig. 3*A*). As expected, a robust and sustained circadian rhythm of luminescence was found in SCN tissue over the 7-day period, consistent with similar studies using *mPer1* promoter fragments to drive Luc expression in transgenic animals (7, 17, 18). In all such static cultures, there was a gradual damping of the circadian amplitude, which is likely caused by the depletion of both nutrients and luciferin during the 7-day interval because the medium was not changed. In contrast to that seen in *mPer1*::*Luc* transgenic animals, however, peripheral tissues in *mPer2*^{Luc} mice expressed robust and persistent circadian oscillations in luminescence (Fig. 3*A*). Particularly robust circadian oscillations were seen in cornea, liver, pituitary, retrochiasmatic area, lung, and tail.

Using the peak of the circadian oscillation in luminescence during the interval between 12 and 36 h in culture, we constructed phase maps for the SCN and peripheral tissues (Fig. 3*B*). Peak PER2::LUC expression occurred at circadian time 12 in the SCN, which is identical to that seen *in vivo* (13). All of the peripheral tissues exhibited delayed phase relationships relative to the SCN [ANOVA, F (6,21) = 7.19, P = 0.000285], consistent with that seen at the organismal level (11, 27). For example, the 4-hr phase delay in *mPer2* expression between the SCN and the liver is faithfully reported in *mPer2*^{Luc} mice (11, 27, 28).

In addition to the characteristic phases of PER2::LUC expression in each tissue, there were characteristic circadian periods expressed by different tissues (Fig. 3*C*). Significant differences in mean period were found from tissue to tissue [ANOVA, F (6,21) = 3.02, P = 0.027; Scheffé's post hoc comparison, $P \leq 0.05$], with the shortest period occurring in cornea (22.2 h) and the longest occurring in kidney (24.8 h). Interestingly, the period of the SCN (23.5 h) was the same as that seen for the free-running period of locomotor behavior of these animals in DD (Table 1). The phase differences in the different tissues reported above are not correlated with their endogenous period values (R = 0.00223, P = 0.99), so that other factors besides period length, such as entraining signals or responsiveness to entraining signals, must vary in different tissues. Taken together, the unique circadian phase and period values expressed by each tissue suggest that the quantitative properties of the circadian oscillators in each tissue are unique and tissue specific. Perhaps differences in the cellular milieu and/or the complement of circadian genes expressed in each tissue contribute to the quantitative differences in circadian properties. Moreover, these tissue-specific differences in circadian properties could be a reflection of selective factors on phasing of rhythms in organ systems in a manner analogous to that seen at the organismal level (10, 29).

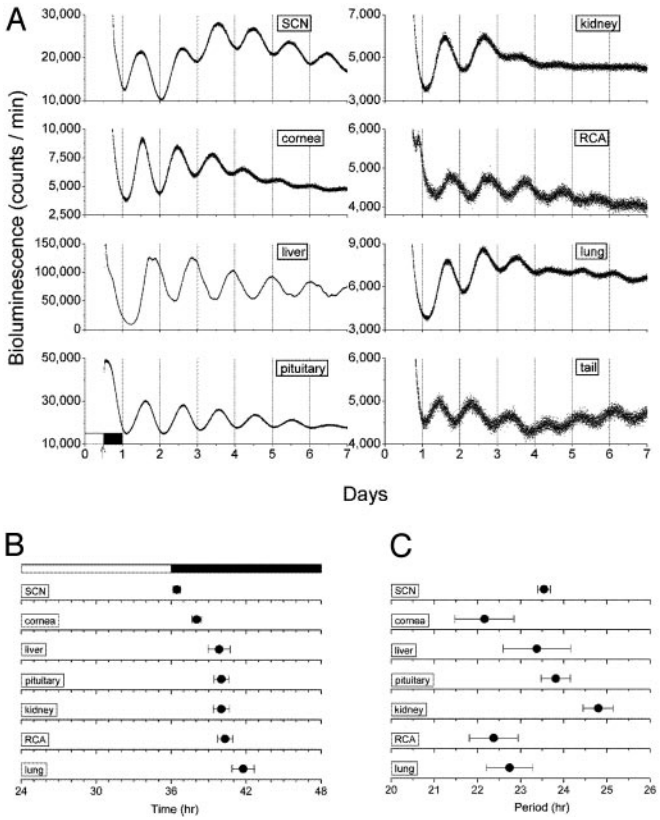

Fig. 3. Real-time analysis of circadian expression of mPER2::LUC. (*A*) Representative records of bioluminescence showing circadian profiles of mPER2 expression from various tissues from *mPer2*^{Luc} knockin animals. Tissues were explanted just before lights off (arrow). Light output (in counts per min) is plotted against previous light onset. (*B*) Phase map for central and peripheral circadian oscillators of *mPer2*^{Luc} knockin mice. The peak of the circadian oscillation was determined during the interval between 12 and 36 h in culture. The average times (± SEM) of peaks were plotted against the time of last lights on (indicated by filled and empty bar). Data for SCN, cornea, liver, pituitary, kidney, retrochiasmatic area (RCA), and lung are shown. (*C*) Period values of mPER2 rhythms in central and peripheral tissues of *mPer2*^{Luc} knockin mice described in *B*. Mean periods (± SEM) for SCN, cornea, liver, pituitary, kidney, RCA, lung and tail are shown.

Persistent Circadian Oscillations of mPER2 Expression in Peripheral Tissues for 20 Days. Because our initial 7-day experiments revealed a robust circadian oscillation in Luc activity in SCN and several peripheral tissues, we maintained some of the explants in culture for >20 days to examine the long-term persistence of oscillations. The cultures were not disturbed in any manner during the experiment (i.e., changing the media or supplementing the cultures with additional luciferin substrate), because such manipulations can reinitiate rhythmicity (7). Unexpectedly, we observed a persistent, self-sustained oscillation in luminescence from the mPER2::LUC fusion protein in liver and lung tissue for the 20-day recording period (Fig. 4). Although a reduction in rhythm amplitude was evident after several cycles, there re-

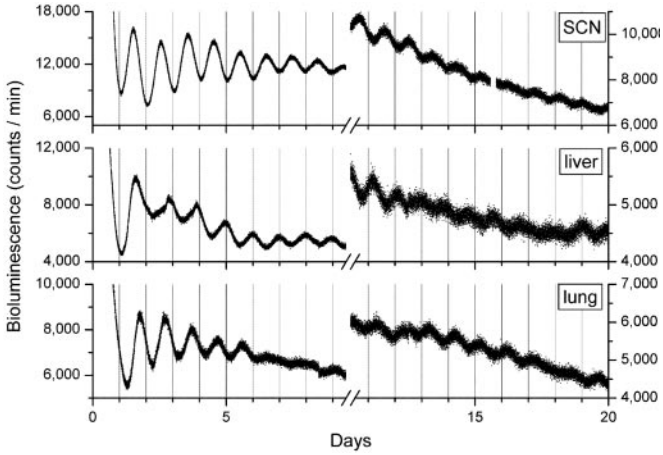

Fig. 4. Long-term persistence circadian rhythms of bioluminescence in peripheral tissues from *mPer2*^{Luc} mice. Bioluminescent measurements from cultures of SCN, liver, and lung tissues were recorded for >20 days without media changes or supplements. The first 10 days (*Left*) and days 11–20 (*Right*) of data are displayed.

mained a discernable circadian rhythm of luminescence in SCN, liver, and lung for the duration of the experiment (note that the amplitude reduction seen is likely caused by the depletion of nutrients and luciferin as described above). Furthermore, the amplitude of the oscillating signals in liver and lung tissues were similar to the signal amplitude observed in SCN tissue.

Lesions of the SCN Do Not Abolish Circadian Rhythms in Peripheral Tissues. Previous work has reported that lesions of the SCN cause a gradual damping and eventual abolition of circadian rhythms of gene expression in peripheral tissues (14, 15, 30–32). To test whether the persistence of PER2::LUC circadian oscillations in peripheral tissues depends on the SCN, we lesioned the SCN in *mPer2*^{Luc} knockin mice and measured the subsequent effects of this procedure on mPER2::LUC expression in peripheral tissues. Successful lesioning of the SCN was confirmed by the loss of circadian rhythms of locomotor activity in mice maintained in DD (Fig. 5*A*). Peripheral tissues were collected from lesioned animals showing completely arrhythmic locomotor activity rhythms and from SCN-intact, control animals showing normal locomotor activity and placed in static explant cultures. Contrary to previous work, SCN lesions did not abolish circadian rhythms of *mPer2* expression in any of the peripheral tissues examined (Fig. 5*B*). Indeed, particularly robust rhythms in luminescence were seen for >7 days in cornea, pituitary, and lung tissues. Additionally, we continued to record Luc activity in liver cultures of intact and SCN-lesioned mice for 14 days without changing the media (Fig. 5*C*). The amplitude of the rhythm from SCN-lesioned mice was not different compared to intact controls. Upon changing the media on day 14, we observed an increase in amplitude of circadian rhythms of Luc activity in liver cultures both from intact and SCN-lesioned animals. These findings corroborate our previous results suggesting that peripheral tissues contain the molecular components required for SCN-independent, persistent circadian oscillation. Furthermore, the results make it highly unlikely that the persistent peripheral circadian rhythms arose from a residual rhythm-sustaining effect of the SCN because SCN-lesioned animals were maintained in constant conditions for 3–5 weeks before tissue removal.

We next examined the effects of SCN lesions on the phases of the rhythms of peripheral tissues by constructing phase plots as before (Fig. 6*A*). In SCN-intact control animals maintained in LD12:12 and DD conditions, the phase PER2::LUC both within

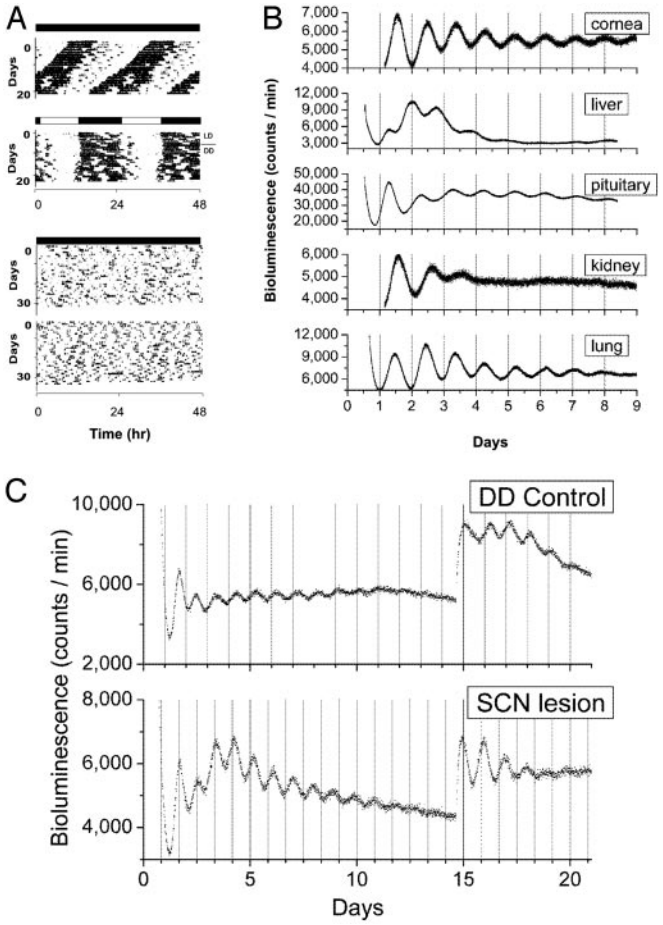

Fig. 5. Real-time analysis of circadian expression of mPER2::LUC protein in peripheral tissues of SCN-lesioned *mPer2*^{Luc} knockin animals. (*A*) Representative locomotor activity records for two intact control (*Upper*) and two SCN-lesioned *mPer2*^{Luc} knockin (*Lower*) animals maintained in DD. Complete loss of circadian locomotor activity rhythm is evident in the SCN-lesioned mice. (*B*) Bioluminescent measurements from static explant cultures of cornea, liver, pituitary, kidney, and lung tissues from SCN-lesioned *mPer2*^{Luc} mice maintained in DD. A self-sustained circadian rhythm of bioluminescence in peripheral tissues, equivalent to that observed in nonlesioned *mPer2*^{Luc} knockin animals (Fig. 3*A*), is evident here in SCN-lesioned *mPer2*^{Luc} knockin peripheral tissues. Missing data between days 0.5 and 1.2 in cornea and kidney records were the result of a computer malfunction. (*C*) Circadian oscillation of liver explants from intact control (DD) and SCN-lesioned mice. After 14 days of culture, media were replaced and circadian oscillation was reinitiated in liver explants from both intact and SCN-lesioned mice.

and among animals is clustered and consistent with our previous experiments (Fig. 3*B*). In SCN-lesioned animals, however, there was a significant dispersion of phase in liver, pituitary, kidney, and lung tissues within and among animals (Fig. 6*A Bottom*). We observed a main effect of tissue on time of peak luminescence [ANOVA, F (4,115) = 6.21, P = 0.000147], and a main effect of SCN lesions, with lesioned animals differing significantly both from LD and DD controls [ANOVA, F (2,115) = 22.95, P = 0; Tukey–Kramer post hoc comparison, $P \leq 0.05$]. SCN lesions disrupted phase synchrony even from tissue to tissue within individual animals, which is a form of "internal desynchronization." These results suggest that although the SCN is not required for persistent circadian rhythms of mPER2::LUC bioluminescence in peripheral tissues, it does, however, serve to coordinate phase among the peripheral tissues within individuals. The exception among the peripheral tissues examined was the cornea in which phase coordination was maintained in

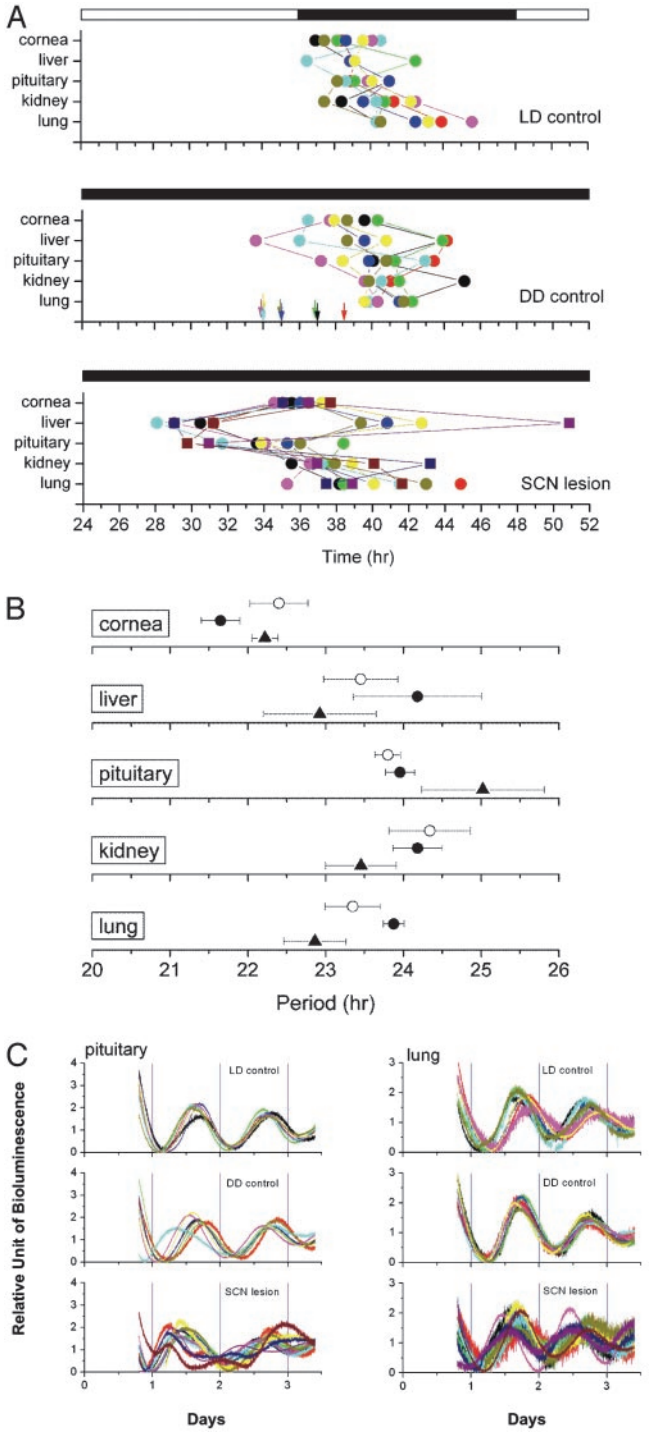

Fig. 6. Phase and period maps of SCN-lesioned mice. (*A*) (*Top*) Phase map of peripheral oscillators in *mPer2*^{Luc} LD control mice ($n = 8$). (*Middle*) Phase map of peripheral oscillators in *mPer2*^{Luc} DD control mice ($n = 8$). Arrows represent activity onset for each animal. (*Bottom*) Phase map of peripheral oscillators in *mPer2*^{Luc} SCN-lesioned mice ($n = 11$). The average times (± SEM) of peaks were plotted against the time of last lights on. Each animal is represented by a colored symbol, and tissues from the same animal are connected by lines. Circles represent 12 and 16 days in DD; squares represent 32 days in DD. (*B*) Circadian period values of mPER2::LUC rhythms in LD control mice (○), DD control mice (●), and SCN-lesioned mice (▲). Mean periods (± SEM) for cornea, liver, pituitary, kidney, and lung are shown. (*C*) Superimposed plots of bioluminescent data from pituitary and lung for all animals including LD controls, DD controls, and SCN-lesioned mice. The first three cycles in culture are represented; each animal's record is of a different color. Phase desynchronization is evident in individual records of the SCN-lesioned animals for both tissues.

SCN-lesioned mice. Because the cornea is within the eye and may have access to photic entrainment from the retina, this tissue could have been entrained by light. The eye is unique in the mammalian circadian system as the only tissue that can be entrained by light independently from the SCN (6, 33).

In contrast to the phase differences observed in SCN-lesioned mice, circadian period values for each tissue were not affected by SCN lesions, and the tissue-specific period differences observed in normal mice were preserved in SCN-lesioned mice [main effect for tissue, ANOVA, F (4,113) = 10.96, $P = 0$; Tukey-Kramer post hoc comparison, $P \leq 0.05$] (Fig. 6*B*). Thus, although the phase relationships of the tissues within and between animals were disrupted in SCN-lesioned animals, each tissue maintained a characteristic period, suggesting that the phase desynchrony was not caused by SCN lesion-induced period changes.

To illustrate the phase desynchrony in more detail, we highlight two tissues, pituitary and lung, which have particularly clear circadian rhythms of PER2::LUC expression (Fig. 6*C*). From composite records showing individual records superimposed, it is clear that among the control animals in both LD and DD conditions, phase coordination is maintained as seen by the coherence among records from individual animals. The records from the tissues of the SCN-lesioned animals, on the other hand, are strikingly different. There is an obvious asynchrony of phase from record to record both in pituitary and lung among SCN-lesioned mice. Taking the ensemble average of the desynchronized rhythms leads to an apparent reduction in amplitude and loss of rhythm across the group of SCN-lesioned animals. Thus, population sampling experiments of SCN-lesioned mice would be expected to have reduced amplitude as a consequence of desynchrony rather than loss of rhythmicity at the level of individual animals/tissues.

Is the SCN a Master Synchronizer, Rather than a Driver, of Peripheral Circadian Oscillators? The mammalian circadian system is thought to be composed of a hierarchical set of oscillators with the SCN acting as a master pacemaker that drives downstream peripheral oscillators (34–38). Current dogma holds that the SCN contains self-sustained circadian oscillators and that peripheral oscillators contain damped oscillators (4, 7, 10, 37–40). Using *mPer1*::*Luc* transgenic animals, previous studies have shown that, whereas *ex vivo* cultures of SCN tissue continue to express a self-sustained circadian rhythm of bioluminescence for >30 days, rhythms in peripheral tissues rapidly damp after two to seven cycles (7). The *mPer1*::*Luc* transgenic results support the view that the SCN represents the master mammalian circadian pacemaker that is able to both generate its own self-sustained circadian rhythms and sustain circadian rhythmicity in damped peripheral oscillators (7). By contrast, using a PER2::LUC fusion protein reporter, we show here that both the SCN and peripheral tissues from *mPer2*^{Luc} knockin mice express long-term persistent circadian rhythms of bioluminescence. Furthermore, we show that individual tissues isolated in culture exhibit unique circadian period and phase properties, suggesting that the quantitative characteristics of circadian oscillators are tissue specific. Finally, our results from the *mPer2*^{Luc} knockin mice suggest that peripheral tissues contain persistent circadian oscillators that do not depend on the SCN. It could be argued that our findings represent after-effects of peripheral tissue exposure to SCN output *in vivo* just before PMT testing. To test this possibility directly, we lesioned the SCN of *mPer2*^{Luc} knockin mice, allowed the animals to recover in DD for several weeks, and measured circadian bioluminescence from *ex vivo* cultures from several peripheral organs. We reasoned that should the SCN be required to sustain circadian rhythmicity in the peripheral tissues, lesioning this structure followed by several weeks of recovery in constant conditions before removal of tissues, would reveal damped or absent circadian oscillations upon PMT analysis of cultured peripheral tissues. After ablation of the SCN, others have reported a complete loss of rhythmic clock gene expression or

a significant damping of clock gene expression (14, 15, 30, 31). Remarkably, in all tissues examined we again observed persistent, circadian oscillations of mPER2::LUC fusion protein in SCN-lesioned mice for >7 days, confirming our previous findings. After analyzing circadian phase in SCN-lesioned animals and intact controls, we identified a significant effect of lesioning: a striking asynchrony of phase occurred in peripheral tissues within and among animals. Our findings specify the role of the SCN as a phase coordinator, preventing internal desynchronization among persistently rhythmic peripheral clocks with tissue-specific periods, rather than as a pacemaker driving peripheral oscillations.

At first glance, our results raise several questions. First, why were self-sustained peripheral oscillators not revealed by *mPer1*::*Luc* and *mPer1*::*GFP* transgenic studies (7, 8, 16, 17, 24, 25)? The most likely explanations concern the promoter fragments used to construct the *mPer1*-reporter transgenic lines. First, it is possible that the *mPer1* promoter fragments used lacked necessary enhancer elements for persistent circadian oscillations in peripheral tissues. Second, the robust circadian rhythms that we observe in peripheral tissues of the $mPer2^{Luc}$ knockin animals and the lack of persistent rhythmicity in the same tissues of *mPer1*::*Luc* transgenic mice may relate to differences in fusion protein reporters as opposed to RNA reporters, respectively. That is, posttranscriptional regulation in the $mPer2^{Luc}$ knockin animals may be necessary to produce the observed self-sustained circadian rhythms in peripheral tissues. In the *mPer1*::*Luc* mice posttranscriptional regulation would not be apparent because the *mPer1* promoter fragment simply drives the expression of Luc as opposed to an mPER1::LUC fusion protein. Third, as in all transgenic studies, the possibility of position effects must be taken into consideration, as transgenes are subject to random integration. This idea is less likely to pertain in the present case, however, given that several independent laboratories have generated *mPer1*-reporter transgenic animals and report similar results. Finally, it is possible that *mPer1* and *mPer2* are regulated differently in peripheral tissues. Under conditions of *ex vivo* culture, it is possible that the *mPer1* locus is more susceptible to damping than the *mPer2* locus.

A second important question raised by the results presented here is why other studies did not demonstrate robust circadian oscillations in peripheral tissues after SCN lesions. We believe that this may in part relate to the fact that in some of those studies population sampling of RNA obtained from peripheral tissues of several SCN-lesioned animals at different time points was used to assay circadian rhythmicity. With our method, it is possible to examine tissue explants from several organs from the same animal, continuously in real time. Thus, we obtain data for each animal and each tissue continuously over many cycles. From the plots of our raw bioluminescence data and analyses of phase, both of which reveal a clear desynchronization of phase from tissue to tissue within and among SCN-lesioned animals (Fig. 6 *A* and *C*), it is apparent that, had we taken tissues from groups of animals at each of several time points and averaged the data there would have been apparent damping of rhythmicity.

A critical issue that remains to be resolved, however, is whether circadian rhythms in SCN-lesioned mice persist *in vivo*. Because our *ex vivo* experiments cannot be assumed to reflect the *in vivo* state of the tissue, this question remains open. The phase dispersion of circadian rhythms seen in SCN-lesioned mice, however, suggests that peripheral organs are likely to be "free-running" in the absence of the SCN, and that the phase dispersion seen *ex vivo* is a reflection of the *in vivo* phase. If, on the other hand, the *ex vivo* phase of the rhythm was initiated by the time of explant, one would expect all of the cultures to have similar clustered phases as was seen in the intact LD and DD control mice. Because the phases in SCN-lesioned mice were dispersed, logically the only other explanation would be that the explant procedure differentially affects SCN-lesioned vs. control tissue phases.

In future work, it will be important to develop methods to measure peripheral circadian rhythms longitudinally in individual mice because as discussed above SCN lesion-induced phase desynchrony of peripheral rhythms can compromise the interpretation of typical circadian population sampling experiments. Only under these conditions will it be possible to determine definitively whether the *ex vivo* results reported here are an accurate reflection of the situation *in vivo*.

On the Significance of Persistent Peripheral Circadian Oscillators. The discovery by Schibler and colleagues (9) that a serum shock can induce circadian rhythms of gene expression in Rat-1 fibroblasts, an immortalized cell line cultured for years in the absence of SCN contact, was remarkable and heralded a new era. In a commentary accompanying that paper, Rosbash (41) suggested the provocative idea that Rat-1 fibroblasts should replace the SCN as a model system for studying circadian mechanisms. Until now, Rosbash's assertion has been discounted because the SCN was considered to be qualitatively different and therefore superior to any other tissue. The persistence of circadian oscillations in peripheral tissues reported here is significant for at least two major reasons. First, the supremacy of SCN tissue as the only persistent circadian oscillator no longer holds. Importantly, this means that mechanistic insight gleaned from experimentally tractable cells and tissues such as hepatocytes and cell lines will likely apply generally to all circadian oscillators. Second, the existence of circadian oscillations in tissues that persist for >20 cycles demands that synchronization mechanisms must exist in these peripheral tissues to maintain coherent oscillations. Because persistent circadian oscillations were observed in a wide variety of tissues and organs, it appears likely that cell- and organ-specific synchronization mechanisms must exist. For example, in organs such as the lung, liver, and kidney, what signaling mechanisms might be used to maintain synchrony within each tissue?

In summary, our results demonstrate that individual peripheral tissues contain circadian oscillators capable of persistent rhythmicity for up to 20 days independent of SCN input. Under *ex vivo* culture conditions, unique circadian phase and period properties of individual tissues from different organs are revealed. *In vivo* then, the SCN function more to coordinate the appropriate phase relationships among peripheral tissues than to drive the circadian rhythms in cells of those tissues. Using the $mPer2^{Luc}$ reporter animals described here, it should be possible to develop methods to study the circadian properties of peripheral tissues at the level of single cells and define further the role of the SCN in relation to peripheral clocks.

We thank Choogon Lee and Jui-Ming Lin for helpful discussions and technical assistance; Lynn Doglio for performing ES cell microinjections; Alexandra L. Joyner for providing the floxed Neo cassette and W4 ES cells; Martha H. Vitaterna for assisting with statistical analyses; and members of the Takahashi, Menaker, and Yoo laboratories for discussions and suggestions. J.S.T. is an Investigator in the Howard Hughes Medical Institute. This work was supported in part by the National Science Foundation Center for Biological Timing, National Institutes of Health Grant MH56647 (to M.M.), and the Korea Advanced Institute of Science and Technology (O.J.Y.).

1. Ralph, M. R., Foster, R. G., Davis, F. C. & Menaker, M. (1990) *Science* **247,** 975–978.
2. Weaver, D. R. (1998) *J. Biol. Rhythms* **13,** 100–112.
3. Takahashi, J. S., Turek, F. W. & Moore, R. Y. (2001) *Handbook of Behavioral Neurobiology: Circadian Clocks* (Plenum, New York), Vol. 12.
4. Reppert, S. M. & Weaver, D. R. (2002) *Nature* **418,** 935–941.
5. Plautz, J. D., Kaneko, M., Hall, J. C. & Kay, S. A. (1997) *Science* **278,** 1632–1635.
6. Tosini, G. & Menaker, M. (1996) *Science* **272,** 419–421.
7. Yamazaki, S., Numano, R., Abe, M., Hida, A., Takahashi, R., Ueda, M., Block, G. D., Sakaki, Y., Menaker, M. & Tei, H. (2000) *Science* **288,** 682–685.

8. Abe, M., Herzog, E. D., Yamazaki, S., Straume, M., Tei, H., Sakaki, Y., Menaker, M. & Block, G. D. (2002) *J. Neurosci.* **22,** 350–356.
9. Balsalobre, A., Damiola, F. & Schibler, U. (1998) *Cell* **93,** 929–937.
10. Schibler, U., Ripperger, J. & Brown, S. A. (2003) *J. Biol. Rhythms* **18,** 250–260.
11. Zylka, M. J., Shearman, L. P., Weaver, D. R. & Reppert, S. M. (1998) *Neuron* **20,** 1103–1110.
12. Lee, C., Etchegaray, J. P., Cagampang, F. R., Loudon, A. S. & Reppert, S. M. (2001) *Cell* **107,** 855–867.
13. Field, M. D., Maywood, E. S., O'Brien, J. A., Weaver, D. R., Reppert, S. M. & Hastings, M. H. (2000) *Neuron* **25,** 437–447.
14. Akhtar, R. A., Reddy, A. B., Maywood, E. S., Clayton, J. D., King, V. M., Smith, A. G., Gant, T. W., Hastings, M. H. & Kyriacou, C. P. (2002) *Curr. Biol.* **12,** 540–550.
15. Sakamoto, K., Nagase, T., Fukui, H., Horikawa, K., Okada, T., Tanaka, H., Sato, K., Miyake, Y., Ohara, O., Kako, K. & Ishida, N. (1998) *J. Biol. Chem.* **273,** 27039–27042.
16. Kuhlman, S. J., Quintero, J. E. & McMahon, D. G. (2000) *NeuroReport* **11,** 1479–1482.
17. Yamaguchi, S., Mitsui, S., Miyake, S., Yan, L., Onishi, H., Yagita, K., Suzuki, M., Shibata, S., Kobayashi, M. & Okamura, H. (2000) *Curr. Biol.* **10,** 873–876.
18. Wilsbacher, L. D., Yamazaki, S., Herzog, E. D., Song, E. J., Radcliffe, L. A., Abe, M., Block, G., Spitznagel, E., Menaker, M. & Takahashi, J. S. (2002) *Proc. Natl. Acad. Sci. USA* **99,** 489–494.
19. Antoch, M. P., Song, E. J., Chang, A. M., Vitaterna, M. H., Zhao, Y., Wilsbacher, L. D., Sangoram, A. M., King, D. P., Pinto, L. H. & Takahashi, J. S. (1997) *Cell* **89,** 655–667.
20. Vitaterna, M. H., King, D. P., Chang, A. M., Kornhauser, J. M., Lowrey, P. L., McDonald, J. D., Dove, W. F., Pinto, L. H., Turek, F. W. & Takahashi, J. S. (1994) *Science* **264,** 719–725.
21. Shimomura, K., Low-Zeddies, S. S., King, D. P., Steeves, T. D., Whiteley, A., Kushla, J., Zemenides, P. D., Lin, A., Vitaterna, M. H., Churchill, G. A. & Takahashi, J. S. (2001) *Genome Res.* **11,** 959–980.
22. Sokolove, P. G. & Bushell, W. N. (1978) *J. Theor. Biol.* **72,** 131–160.
23. Takahashi, J. S. & Menaker, M. (1982) *J. Neurosci.* **2,** 815–828.
24. Stokkan, K. A., Yamazaki, S., Tei, H., Sakaki, Y. & Menaker, M. (2001) *Science* **291,** 490–493.
25. Yamazaki, S., Straume, M., Tei, H., Sakaki, Y., Menaker, M. & Block, G. D. (2002) *Proc. Natl. Acad. Sci. USA* **99,** 10801–10806.
26. Zheng, B., Larkin, D. W., Albrecht, U., Sun, Z. S., Sage, M., Eichele, G., Lee, C. C. & Bradley, A. (1999) *Nature* **400,** 169–173.
27. Damiola, F., Le Minh, N., Preitner, N., Kornmann, B., Fleury-Olela, F. & Schibler, U. (2000) *Genes Dev.* **14,** 2950–2961.
28. Panda, S., Antoch, M. P., Miller, B. H., Su, A. I., Schook, A. B., Straume, M., Schultz, P. G., Kay, S. A., Takahashi, J. S. & Hogenesch, J. B. (2002) *Cell* **109,** 307–320.
29. Pittendrigh, C. S. (1981) in *Handbook of Behavioral Neurobiology: Biological Rhythms*, ed. Aschoff, J. (Plenum, New York), Vol. 4, pp. 57–80.
30. Terazono, H., Mutoh, T., Yamaguchi, S., Kobayashi, M., Akiyama, M., Udo, R., Ohdo, S., Okamura, H. & Shibata, S. (2003) *Proc. Natl. Acad. Sci. USA* **100,** 6795–6800.
31. Iijima, M., Nikaido, T., Akiyama, M., Moriya, T. & Shibata, S. (2002) *Eur. J. Neurosci.* **16,** 921–929.
32. Hara, R., Wan, K., Wakamatsu, H., Aida, R., Moriya, T., Akiyama, M. & Shibata, S. (2001) *Genes Cells* **6,** 269–278.
33. Berson, D. M. (2003) *Trends Neurosci.* **26,** 314–320.
34. Meijer, J. H. & Rietveld, W. J. (1989) *Physiol. Rev.* **69,** 671–707.
35. Klein, D. C., Moore, R. Y. & Reppert, S. M. (1991) *Suprachiasmatic Nucleus: The Mind's Clock* (Oxford Univ. Press, New York).
36. Moore, R. Y. (1997) *Annu. Rev. Med.* **48,** 253–266.
37. Buijs, R. M. & Kalsbeek, A. (2001) *Nat. Rev. Neurosci.* **2,** 521–526.
38. Hastings, M. H., Reddy, A. B. & Maywood, E. S. (2003) *Nat. Rev. Neurosci.* **4,** 649–661.
39. Young, M. W. & Kay, S. A. (2001) *Nat. Rev. Genet.* **2,** 702–715.
40. Roenneberg, T. & Merrow, M. (2003) *Curr. Biol.* **13,** R198–R207.
41. Rosbash, M. (1998) *Cell* **93,** 917–919.